Current Applied Science and Technology Vol. 22 No. 3 (May-June 2022)

Research article

Strategies for Metallizing and Electroplating Biodegradable PLA

Varintorn Srisupornwichai[1], Chuanchom Aumnate[2], Patama Visuttipitukul[1], Stephan T. Dubas[3], Martin Metzner[4], Manfred Zinn[5] and Yuttanant Boonyongmaneerat[2]*

[1]*Department of Metallurgical Engineering, Faculty of Engineering, Chulalongkorn University, Bangkok, Thailand*
[2]*Metallurgy and Materials Science Research Institute, Chulalongkorn University, Bangkok, Thailand*
[3]*Petroleum and Petrochemical College, Chulalongkorn University, Bangkok, Thailand*
[4]*Fraunhofer Institute for Manufacturing Engineering and Automation IPA, Stuttgart, Germany*
[5]*Institute of Life Technologies, University of Applied Sciences and Arts Western Switzerland (HES-SO Valais-Wallis), Sion, Switzerland*

Received: 2 June 2021, Revised: 30 August 2021, Accepted: 28 September 2021

DOI: 10.55003/cast.2022.03.22.013

Abstract

Keywords

poly(lactic acid);

metallizing;

electroplating;

plating-on-plastic;

fused deposition modelling 3d-printing technique

With environmental awareness in societies, bioplastics continue to receive increasing attention and utilization rate. Polylactic acid (PLA) is one of the most important biopolymers in the market today, owing to its high strength and relative ease of forming. Unlike the common structural, fossil fuel-based plastics, such as Acrylonitrile-Butadiene-Styrene (ABS), the surface of PLA cannot be readily metallized in preparation for electroplating using the conventional plating-on-plastic (POP) process. This partially limits the wider use of the material for functional and decorative applications. In this research study, we systematically explored three strategies for metallizing the surface of PLA, namely, (A) chemical etching and palladium activation technique, (B) polyelectrolyte multilayers (PEMs) and Ag nanoparticle deposition technique, and (C) Ag conductive painting technique. PLA samples, prepared by Fused Deposition Modelling (FDM) 3D-printing technique, were metallized by various techniques followed by electroless deposition and electroplating of copper layers. The study was performed comparatively with respect to the ABS surface. The samples microstructures, chemical distributions, and plating characteristics were assessed with optical and scanning electron microscopy. The adhesion of the metallic coatings was analyzed using scratch test and tape test. Although uniform deposition of copper layers on PLA surfaces could be achieved using all three metallizing methods under investigation, the three methods were found to provide different degrees of benefits with respect to deposition rate, surface uniformity, and process simplicity.

*Corresponding author: Tel.: (+66) 22184243 Fax: (+66) 26117586
E-mail: yuttanant.b@chula.ac.th

1. Introduction

Metallization on a non-conductive surface such as plastics can be achieved using several techniques, including spraying metal, conductive inkjet printing, chemical vapor deposition, metal sputtering, and electroless plating, all of which can provide a metal layer for functional and decorative purposes [1-4]. Among the various metallization techniques for plastics, electroless plating is an outstanding technique as it provides layer uniformity even for intricate objects and can be employed in mass production [5]. Furthermore, there is no need for an external electrical potential during electroless plating because it relies on the oxidation-reduction reaction on the activated plastic surface [2, 3, 6, 7]. Electroless plating is usually followed by electroplating to add a variety of metal layers such as copper, nickel, chromium, and gold onto the electroless plated layer or to build up metal thickness. This process is known as plating on plastics (POP). Recently, the development of sustainable POP processes has become significant for broad industrial markets ranging from cosmetic packaging, decorative products, electronics components, sanitary parts, automotive parts, aerospace and electro-magnetic interference shielding [1, 8-10].

The traditional POP process consists of surface pre-treatment (chemical etching, sensitizing and activating) to render micro-porosities and deposit catalytic nuclei on the porous surface. The surface pre-treatment process generally generates hazardous substances, such as CrO_3, to the environment, and lead to increasing wastewater treatment costs [7, 10, 11]. Moreover, the necessity of using precious metals such as palladium that served as catalytic nuclei is costly, thus raising the cost of POP products [1, 8-10, 12, 13]. Normally, POP products are based on fossil-fuel derived plastics, such as acrylonitrile-butadiene-styrene (ABS), polycarbonate (PC), polyetherimide (PEI), which are not quite sustainable for the environment [14]. Furthermore, increasing future demands for POP products such as lighter automotive parts, new materials such as bioplastics that are renewable will become increasingly in demand. Waste reduction and materials recoverability are among additional important benefits gained from using such environmentally-friendly materials.

Polylactic acid (PLA) [15-20] is an aliphatic polyester derived from renewable resources and agricultural products, such as corn, sugar beet, wheat and sugarcane. It offers a number of advantages, including renewability, rigidity, high strength, low density, biodegradability [21], and low CO_2 emission [22]. Generally, PLA can be processed by various techniques such as injection molding, blow molding, thermoforming, and three-dimensional (3D printing). Fused Deposition Modelling (FDM) is among the current 3D printing methods that have gained much attention for part fabrication with PLA and ABS. The two are now well-known thermoplastic filaments used as feedstock for FDM 3D printing [23]. However, PLA appears in few studies in relation to POP, partly due to challenges associated with its low glass transition temperature and high sensitivity to hydrolysis reaction, which can lead to deformation and degradation of parts during the POP process [2, 3, 24-28]. Thus, developing a suitable POP process and optimizing appropriate POP parameters for PLA are critical challenges for researchers in the field. From literature reviews, some surface metalizing processes for the electroplating of non-ABS plastics have been proposed. These include supercritical carbon dioxide assisted impregnation of activator [29], chemical etching and activation [24], hydrogel coating and metal nanoparticle activation [30], polyelectrolyte multilayer (PEMs) and metal nanoparticle deposition [31, 32], and conductive coating [33-38]. Many of these processes are not readily applicable for metalizing PLA owing to its low glass transition temperature. Furthermore, in-depth and systematic studies that specifically investigate and analyze the applicability of the metallizing processes for PLA are very limited.

In this research, low-temperature pre-treatment techniques for plating on PLA were comparatively investigated, including (A) chemical etching and palladium activation, (B) PEM and silver nanoparticle (NP) deposition, and (C) silver conductive painting. The metallized PLA samples, which were subsequently electrodeposited with copper, were analyzed with respect to

platability, coating uniformity, and layer adhesion. The results were systematically compared to the conventional POP process with ABS. The knowledge gained from this work opens an opportunity for surface improvement of PLA that may be applied to some specific needs, and also provides fundamental understanding of how to effectively metallize other biopolymers of unique characteristics.

2. Materials and Methods

2.1 Substrate fabrication

Rectangular specimens with the dimension of 2x7x0.2 cm were prepared using FDM 3D printer (Cubicon 3DP-210F). The 3D printing parameters for PLA and ABS are presented in Table 1. In this study, 100% infill density was set for all samples to avoid moisture trapping into the parts during the metallization and plating studies [24].

Table 1. Parameters set up for 3D printing of PLA and ABS

Materials	PLA	ABS
Nozzle temperature (°C)	210	240
Build plate temperature (°C)	60	115
Chamber temperature (°C)	35	55
Infill density (%)	100	100
Print speed (mm/s)	50	50
Layer thickness (mm)	0.2	0.2

2.2 Surface pre-treatment

The surfaces of 3D printed parts were pre-treated via three strategies including (A) chemical etching and Pd activation, (B) PEM and Ag NP deposition, and (C) Ag conductive painting technique. The schematic illustrations of each strategy are shown in Figure 1.

2.2.1 Polylactic acid (PLA)

2.2.1.1 Sample group A: Chemical etching and Pd activation

The method used was similar to the conventional metallization of ABS, but the process was modified in the etching step using more benign chemicals and temperature. PLA samples were chemically-etched in 200 g/l KOH solution at 45°C for 40 min [24]. The etched PLA samples were then sensitized in $SnCl_2$ solution for 7 min, activated in $PdCl_2$ solution for 3 min at room temperature, and then rinsed with DI water. The catalytic Pd atoms formed and served as reactive sites for the electroless deposition reaction to take place, whereby metal ions are reduced to metallic deposits [39].

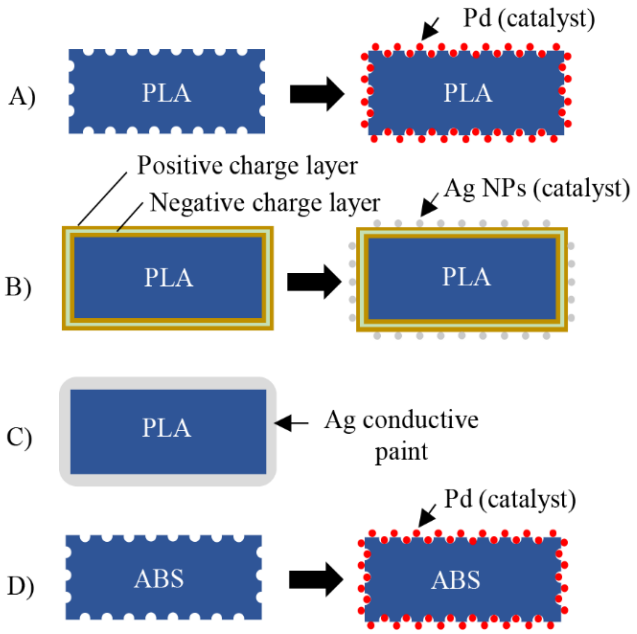

Figure 1. Schematic diagrams of different surface metallizing pre-treatment strategies: (A) chemical etching and Pd activation (PLA), (B) PEMs and Ag NPs deposition (PLA), (C) Ag conductive painting (PLA), and (D) chemical etching and Pd activation benchmark (ABS benchmark)

2.2.1.2 Sample group B: PEMs and Ag NP deposition

This technique allows metallization at room temperature; hence it is compatible with PLA. Furthermore, it potentially provides the benefits of uniform thickness and good part profile tolerance since only few layers of nanoparticles are deposited to form a thin coating (in nm range). The surface of the PLA sample was first modified via the layer-by-layer (LBL) technique at room temperature to create a polyelectrolyte multilayer that acted as a primer [40] to immobilize and anchor the catalyst. Ag was used herein as the source of catalytic particles, instead of Pd, in order to control the cost of production which is a critical factor when the process is to be scaled-up.

Here the PLA surface was modified using UV light (wavelength of 172 nm) treatment in a chamber for 30 min to increase the wettability. The polyelectrolyte multilayers (PEMs) were deposited via the layer-by-layer method (LBL), which is based on the sequential deposition of oppositely charged polycation and polyanion. The PEMs were coated by dipping the sample into a 10 mM solution of poly(diallyl dimethyl ammonium chloride) (PDADMAC) for 1 min, followed by a rinse step in de-ionized water. This dipping was then repeated with a 10 mM poly(4-styrene sulfonate sodium salt) (PSS) solution for 1 min at room temperature. The alternate dipping was repeated until reaching 7 layers, after which the outermost layer was PDADMAC, providing a net positive charge on the surface. The samples were then soaked in the Ag NP solution for 24 h at room temperature to complete the deposition of Ag NPs on the surface. Prior to the deposition, the Ag NP solution was prepared by the chemical reduction of silver salt (1 mM $AgNO_3$) with sodium borohydride (5 mM $NaBH_4$) and the use of anionic sodium alginate (5 mM) as a capping agent to prevent nucleation growth and coalescence of the nanoparticles.

2.2.1.3 Sample group C: Ag conductive painting

Strategy C appears to be the simplest technique as only a single step is required before electroplating (i.e. no need for the electroless plating step). The conductive paint, which is composed of binder, solvent and conductive powder such as silver or graphite, is applied onto the parts by various methods, for instance, by brushing, dipping, and spraying [33-38]. This technique can potentially reduce wastewater from the metallization process since it contains no wet-coating process.

In this study, Ag conductive paint was synthesized by mixing Ag powder with ethyl-methacrylate copolymer and acetone according to a proprietary formulation. The conductive paint was applied onto the sample surface by brushing at room temperature, and then it was left to air-dry for at least 1 h.

2.2.2 Acrylonitrile-Butadiene-Styrene (ABS): Conventional technique

ABS sample was used as a benchmark in this research. The surface pre-treatment method was similar to strategy A, but in term of etching, samples were soaked in 400 g/l H_2CrO_4 mixed with 400 g/l H_2SO_4 at 70°C for 15 min according to the POP industry's common practice. Etched ABS samples were then sensitized in $SnCl_2$ solution for 7 min, activated in $PdCl_2$ solution for 3 min at room temperature, and subsequently rinsed with DI water.

2.3 Electroless plating and electroplating of Cu

Electroless Cu plating was performed on the samples treated according to (A), (B) and (D) techniques, as described in sections 2.2.1 and 2.2.2. Cu plating was carried out using a commercial solution comprising 84 vol.% DI water, 10 vol.% THRU-CUP PSY-1A, 4%vol THRU-CUP PSY-1B and 2 vol.% formalin. Each deposition session lasted 4 min and was conducted at the controlled temperature of 35°C.

Subsequently, the samples were electroplated in a copper bath, consisting of 220 g/l $CuSO_4$, 40 ml/l H_2SO_4, 0.06 ml/l HCl, and some organic additives. Electrodeposition was performed with the applied current density of 10 A/dm^2 at room temperature for duration of 15-20 min to achieve comparable layer thickness (25-30 μm) among samples from different groups.

2.4 Characterization

2.4.1 Plating efficiency calculation and resistivity measurement

The plating efficiency consideration in this research consisted of cathodic efficiency (C.E.) and plating rate. The C.E. can be calculated according to Faraday's law as shown in equation (1), W is the weight of metal deposited, where I is current (A), A_w is atomic weight, Z is number of valence electrons, F is Faraday constant (96,485 C/mol), t is plating duration, and C.E. is cathodic efficiency.

$$W = \frac{I \times t \times A_w}{Z \times F} \times C.E. \quad (1)$$

The thickness (h) of deposited materials can be calculated using equation (2), where ρ is metal density (Cu=9.92 g/cm^3) and A is surface area.

$$h = \frac{W}{\rho \times A} \quad (2)$$

The plating rate was calculated by h/t.

2.4.2 Morphology

An optical microscope (HRM-300 series Huvitz, Republic of Korea) was used to observe non-etched and etched surface morphology while a scanning electron microscope (JEOL JSM-IT100, Japan) was employed to characterize the cross-sectional of plated layers.

2.4.3 Adhesion

The adhesion between coating and substrates were investigated qualitatively and quantitatively using tape and scratch tests, respectively. The tape test was performed following the ASTM D3359-17 (method B), using a knife to make a grid pattern on a coated surface (each cut was spaced about 1 mm apart and 11 cuts in each direction were made). Adhesive tape was then placed onto the tested area and pulled at 90°. The results of the damaged film were rated according to the standard.

The scratch test was performed according to the ASTM C1624-05, by utilizing a scratch test machine (Fisherscope ST200) in progressive load mode from 0.5 N to 100 N, using a diamond Rockwell indenter with a radius of 200 µm, and a scratch speed of 2.8 mm/min. The scratch profile was then examined with optical microscopy. Normal force, frictional force and coefficient of friction (COF) values were acquired from the test. The critical loads represented the points at which defect and delamination initiated were determined and analyzed.

3. Results and Discussion

3.1 Platability

3.1.1 Metallizing pre-treatment

3D printed samples were successfully produced with uniform surface and without curvature. As anticipated, the materials (PLA and ABS) were non-conductive, with a measured electrical resistance above $1x10^6$ Ohm. Following the application of metallizing pre-treatment process of strategy A, PLA remained non-conductive but seeding of catalytic Pd according to equation (3) was anticipated.

$$Sn^{2+} + Pd^{2+} \rightarrow Sn^{4+} + Pd \quad (3)$$

Similarly, strategy B provided PLA surfaces with clusters of Ag that were catalytic but did not extensively percolate to yield electrical conductivity on the surface. Samples from groups A and B thus required subsequent electroless plating steps to render conductivity prior to electrodeposition. After the electroless plating step, the PLA samples from groups A and B exhibited electrical resistances of 1.5 and 14 Ohm, respectively. On the other hand, PLA samples from group C showed low resistance following a treatment of conductive paint (18 Ohm). The conductivity of electroless plated surface that showed dependency on a pre-treatment process was very interesting and required

further in-depth analysis. After metallizing pre-treatment, the samples from all groups were ready for copper electroplating.

3.1.2 Plating efficiency

The samples from different groups were successfully plated with copper. Looking closely, however, it was found that the cathodic efficiency (C.E.) [41] and plating rate of copper were largely different among different group of samples as shown in Table 2. Samples from group A exhibited C.E. and plating rate comparable to the ABS benchmark. This was attributed to similar metallizing pre-treatment process applied to these two groups, and the result also suggested that the chemical etching and Pd activation process developed and employed in this work were effective, providing on-par plating efficiency compared to the conventional POP process. The samples from groups B and C exhibited lower C.E. and plating rates. These results correlated well with the relatively high electrical resistance observed in the samples of these two groups.

Table 2. Cathodic efficiency and plating rate of copper electroplated on 3D-printed PLA samples that were prepared by different surface pre-treatment techniques (A, B, and C), compared to those of the ABS benchmark.

Sample	A	B	C	Benchmark
Cathodic efficiency (%)	86.22	56.50	57.61	83.86
Plating rate (μm/min)	1.90	1.25	1.27	1.85

3.2 Sample appearance and microstructures

Figure 2 shows the appearance of the 3D-printed samples in the as-printed and as-plated conditions. As observed, the 3D-printed samples were intact, uniform, and without any curvature. Compared to other traditional plastic fabrication techniques, such as injection molding, the surface of the 3D-printed samples exhibited a higher degree of surface roughness. This could be further reduced by optimizing 3D printing parameters such as printing temperature, air gap, nozzle diameter, and layer height [42]. The copper plated samples of all groups exhibited fairly uniform coating and lustrous surfaces. Upon a closer examination, in some limited areas, small non-coated spots could be observed near groove regions of the 3D printed parts. No non-coated spots were found from the samples in group C, although there appeared to be some small non-leveling contour of the plated copper layer, owing to brushing action for applying the conductive paint. The ABS benchmark is characterized by a uniform, no-defect copper layer on its surface.

Figure 3 compares the surface morphology of PLA and ABS samples before and after the etching step in their respective metalizing pre-treatment processes. It is well-known that the acid-based etching process of ABS for preparing its surface for metallizing results in surfaces containing nano-pores which in turn helped with mechanical interlocking of a subsequent plating layer and a substrate. Such surface structure was evidenced herein and shown in Figure 3D. The PLA samples from group A, which were treated with alkaline-based etching process, showed uniform porous layer after coating. The pores are not as refined as observed in the ABS case, but are in the micro regime (3-5 mm). In this case, they were developed due to the hydrolysis reaction, as shown in equation (4) [24]. It is anticipated that surface roughness from such feature would provide mechanical interlocking in a similar fashion as found in the ABS system.

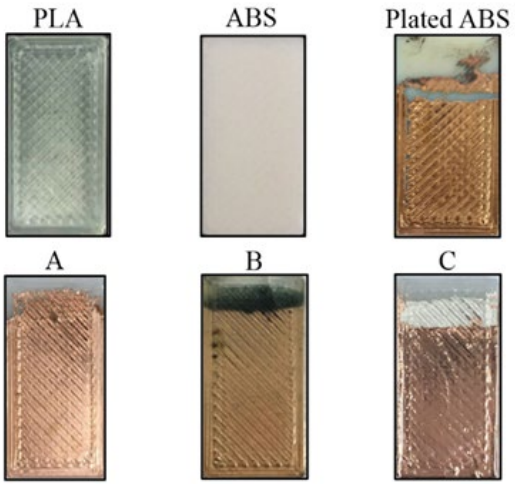

Figure 2. Appearance of the as-printed PLA and ABS 3D-printed samples, as-plated ABS (benchmark), and as-plated PLA samples prepared by different surface pre-treatment strategies: (A) chemical etching and Pd activation, (B) PEMs and Ag NPs deposition, (C) Ag conductive painting

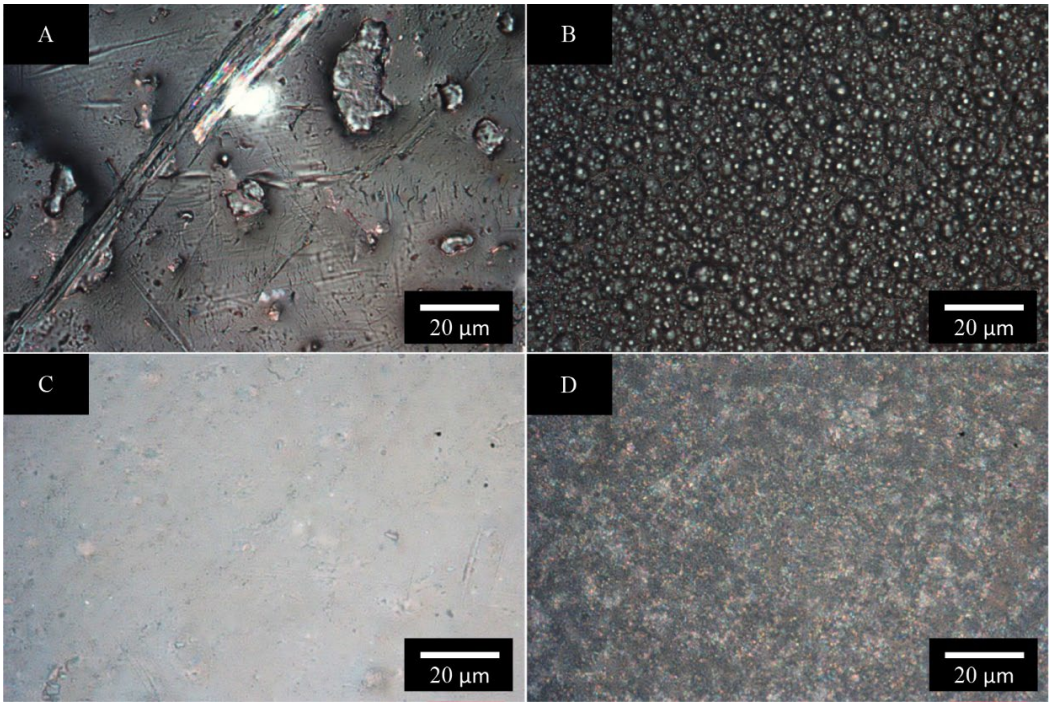

Figure 3. Top-down micrographs of 3D-printed PLA: A) non-etching, B) KOH etching at 45°C for 40 min and ABS, C) non-etching, D) CrO_3 etching at 70°C for 15 min

$$\text{O-CO-O-C-CO-O-} + OH^- \rightarrow \text{-O-CO-OH} + \text{HO-C-CO-O-} \quad (4)$$

Comparing the cross-sectional micrograph of the sample from group A to that of the ABS benchmark (Figure 4A and Figure 4D), it can be clearly seen that the polymer/copper interface is much rougher in the former case. This is parallel to the rougher surface area as indicated in Figure 3B, compared to Figure 3D. Nevertheless, uniform, intact coating layers with no interfacial porosity are observed in both PLA and ABS cases.

The samples from group B were characterized by relatively smooth coating interface and uniform coating layer, as shown in Figure 4B. Along the interface of the copper coating layer lies a stable Ag nanoparticle layer formed by electrostatic attraction between carboxylic moieties from alginate and the quaternary amine of PDAMAC [31, 32, 40]. On the other hand, the samples from group C were characterized by an apparently thick Ag layer between the copper deposit and the polymer substrate. The top surface of the copper coating appears rougher than that found in other groups. Furthermore, the thickness of the copper layer is slightly varied from region to region, due to inconsistency of manual application of the conductive paint.

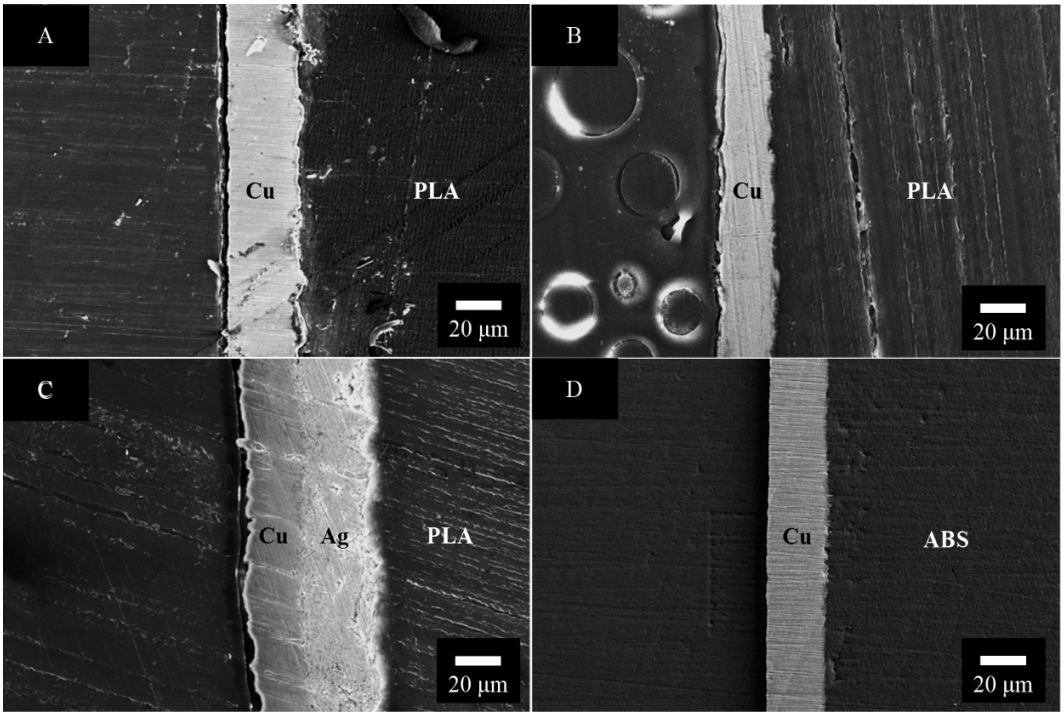

Figure 4. Cross-sectional micrographs of the as-plated PLA samples prepared by different surface pre-treatment strategies: (A) chemical etching and Pd activation, (B) PEMs and Ag NPs deposition, (C) Ag conductive painting, and (D) the plated ABS benchmark

3.3 Coating adhesion

3.3.1 Tape test

The tape test revealed that samples in groups A and C had excellent coating adhesion, with 4B and 5B adhesion classification, respectively. Very minimal coating flaking or peel-off was detected (less than 5%). On the other hand, the coating adhesion of the samples in group B was not as strong, with 1B degree of adhesion. The amount of coating was removed by the tape test as much as 40%. This may be attributed to weak electrostatic interaction at the interface of the samples in this group and to residual stresses developed at the PEMs/metal interface [31, 32]. The relevant prior research on PEMs and electroless deposition demonstrated the importance of the types and properties of PEMs themselves in controlling the adhesion of the polymer film and electroless nickel deposit [31]. It has also been shown that surface treatment of a polymer substrate (PEN and PET) by plasma and UV irradiation provided better film adhesion, unlike UV/ozone exposure [32]. A process to relieve residual stresses developed in the film, such as thermal annealing, may also help improve the adhesive and cohesive strength of the PEM samples. The ABS benchmark investigated in the present study showed relatively high tape test adhesion in the level of 5B.

3.3.2 Scratch test

The samples from groups A and C were then selected for further analysis of coating adhesion quantitatively, using the scratch test technique [42, 43]. Table 3 shows the critical load 1 (Lc_1) and critical load 2 (Lc_2), which represents the loads where cohesive failure and adhesive failure took place, respectively. The coffeciencts of friction corresponding to those points are also presented. The results indicated that Lc_1 of the group C sample was almost twice that of the group A samples, signifying the more intact nature of the plated copper layer in the former group. This may imply that the copper layer of the group C samples had less porosity and/or less residual stresses. Furthermore, Lc_2 of the group C samples was also about twice that of the group A samples. This confirms the higher degree of adhesion of the samples pre-treated with conductive paint. Figure 5 depicts the scratch profiles of the two types of samples, showing what appears to be gross spallation in the group A samples, and buckling spallation in the group C samples. The scratch marks in the group C samples were generally smaller than those of the relevant group A samples.

Table 3. Critical load 1 (Lc_1), critical load 2 (Lc_2), and coefficience of friction (COF) of Cu plated on 3D-printed PLA prepared by different surface pre-treatment strategy evaluated by scratch test method

Sample	Lc_1 (N)	COF_1	Lc_2 (N)	COF_2
A	6.14	0.2	19.49	0.35
C	11.52	0.38	42.65	0.48

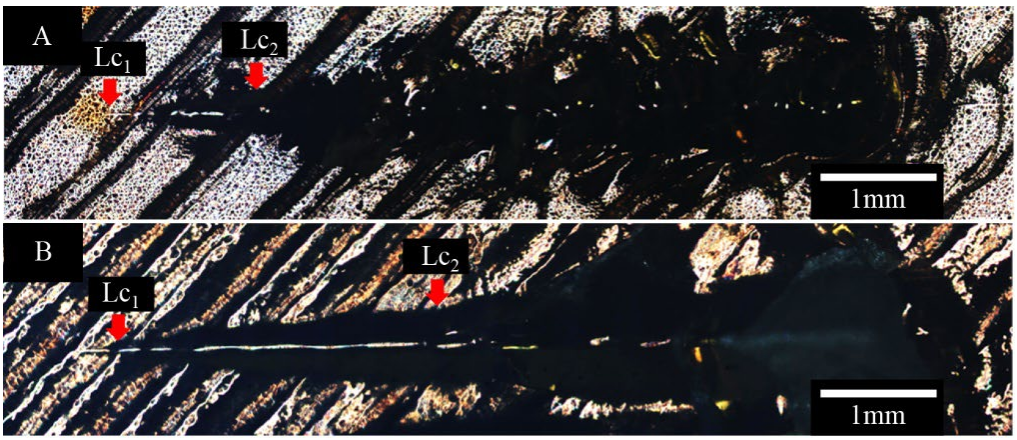

Figure 5. Optical image of damaged scratch profile of PLA sample prepared by: (A) chemical etching and Pd activation (group A), (B) Ag conductive painting (group C)

3.4 Comparison of the three metallizing pre-treatment strategies

The advantages and drawbacks of each metallizing pre-treatment strategies can thus be summarized as follows:

(A) Chemical etching and Pd activation: This technique was similar to traditional surface pre-treatment and resulted in a high plating rate and cathodic efficiency. The high conductivity and strong adhesion were achieved due to the mechanical interlocking mechanism at the interfacial surface between PLA and Cu film. However, the chemicals used in this technique contain precious metal (Pd), which may raise the process cost.

(B) PEMs and Ag NPs deposition: Using Ag as a catalyst instead of Pd, the pre-treatment cost and toxicity were reduced compared to the first strategy. This strategy has a good potential to be applied to bioplastics because the interface is developed with electrostatic interaction, and therefore high-temperature etching is not required. The thickness of the coating layer was uniform along with the interface, and the pre-treatment layer was very thin in the nano-regime which was good for part tolerance. However, plating rate and cathodic efficiency were lower as compared to the first strategy. Furthermore, the adhesion of the copper layer on the substrate was relatively weak.

(C) Ag conductive painting: This is a relatively simple technique for initiating electrical conductivity on the plastic substrate, as it involves only one step before electroplating. Minimization of wastewater and toxicity was anticipated. The results herein revealed that this technique provided a high electrical conductivity for the surface and relatively high adhesion performance. However, non-uniformity of the coating layer and the resulting of thick coating were among some drawbacks that require improvement. Furthermore, if this strategy were to be applied onto a part with intricate geometry, coating application methods other than painting needed to be developed and applied.

These advantages and drawbacks of the 3 strategies can be summarized schematically with respect to five factors, namely plating rate, adhesion performance, part tolerance, environmentally friendliness, mass production capability, as shown in Figure 6.

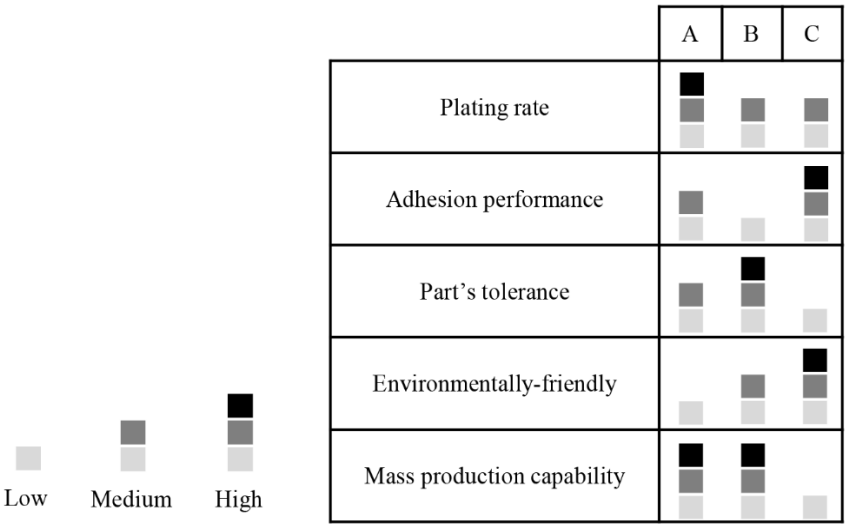

Figure 6. Comparison of degree of advantages of the different metallizing pre-treatment strategies: (A) chemical etching and Pd activation, (B) PEMs and Ag NPs deposition, (C) Ag conductive painting

4. Conclusions

Low-temperature metallization and electrodeposition of Cu was investigated on PLA parts prepared using a fused deposition modelling 3D print machine. Three metallization strategies including (A) chemical etching and Pd activation, (B) PEMs and Ag NPs deposition, and (C) Ag conductive painting, were analyzed and compared. The study revealed that the 3 strategies can generally provide metallizing pre-treatment layers that lead to a fairly uniform deposition of an electroplated copper layer on PLA. The three strategies, however, have different advantages and drawbacks in their current forms. Strategy A provided strong coating and a good coating adhesion, at a relatively high plating rate. A superior part tolerance was anticipated for samples produced by strategy B; however, weak interfacial adhesion was observed. Strategy C was found to be relatively simple and showed a superior coating adhesion, although the coating uniformity and leveling of coating were among challenges that need to be further developed for industrial utilization.

5. Acknowledgements

The authors gratefully acknowledge the funding support from the National Science and Technology Development Agency of Thailand (#P-19-51362), the Southeast Asia – Europe Joint Funding Scheme for Research and Innovation (Project BIOPLATE), German Federal Ministry of Education and Research (BMBF) FKZ 01DP19010 and the Swiss National Science Foundation (IZJFZ2_185638). We sincerely thank Helmut Fischer (Thailand) Co., Ltd. for the support on the scratch test.

References

[1] Horiuchi, S. and Nakao, Y., 2010. Platinum colloid catalyzed etchingless gold electroless plating with strong adhesion to polymers. *Surface and Coatings Technology*, 204(23), 3811-3817.

[2] Equbal, A., Equbal, A. and Sood, A.K., 2014. Metallization on FDM Processed Parts Using Electroless Procedure. *Procedia Materials Science*, 6, 1197-1206.

[3] Equbal, A. and Sood, A.K., 2015. Investigations on metallization in FDM build ABS part using electroless deposition method. *Journal of Manufacturing Processes*, 19, 22-31.

[4] Wang, Y., Cheng, B. and Jing, X., 2013. Adhesion improvement of electroless copper plating on phenolic resin matrix composite through a tin-free sensitization process. *Applied Surface Science*, 271, 303-310.

[5] Tong, J., Su, L., Haraya, K. and Suda. H., 2008. Thin Pd membrane on α-Al_2O_3 hollow fiber substrate without any interlayer by electroless plating combined with embedding Pd catalyst in polymer template. *Journal of Membrane Science*, 310(1), 93-101.

[6] Inagaki, N. and Kimura, H., 2009. Electroless copper plating on acrylonitrile butadiene styrene material surfaces without chromic acid etching and a palladium catalyst. *Journal of Applied Polymer Science*, 111(2), 1034-1044.

[7] Tang, X., Cao, M., Bi, C., Yan, L. and Zhang, B., 2008. Research on a new surface activation process for electroless plating on ABS plastic. *Materials Letters*, 62(6), 1089-1091.

[8] Li, D. and Yang, C.L., 2009. Acidic electroless copper deposition on aluminum-seeded ABS plastics. *Surface and Coatings Technology*, 203(23), 3559-3568.

[9] Bazzaoui, M., Martins, J.I., Bazzaoui, E.A., Albourine, A., Wang, R. and Hong, P.D., 2013. A simple method for acrylonitrile butadiene styrene metallization. *Surface and Coatings Technology*, 224, 71-76.

[10] Luo, L.M., Lu, Z.L., Huang, X.M., Tan, X.Y., Ding, X.Y., Cheng, J.G., Zhu, L. and Wu, Y.C., 2014. Electroless copper plating on PC engineering plastic with a novel palladium-free surface activation process. *Surface and Coatings Technology*, 251, 69-73.

[11] Tengsuwan, S. and Ohshima, M., 2012. Electroless nickel plating on polypropylene via hydrophilic modification and supercritical carbon dioxide Pd-complex infusion. *The Journal of Supercritical Fluids*, 69, 117-123.

[12] Teixeira, L. and Santini, M., 2005. Surface conditioning of ABS for metallization without the use of chromium baths. *Journal of Materials Processing Technology*, 170(1), 37-41.

[13] Tang, X., Bi, C., Han, C. and Zhang, B., 2009. A new palladium-free surface activation process for Ni electroless plating on ABS plastic. *Materials Letters*, 63(11), 840-842.

[14] Skelly, J., 2008. Decorative plating processes for common plastic resins: Resin selection as well as plastic part design is critical to matching the right finishing method with the intended application. *Metal Finishing*, 106(6), 61-65.

[15] Rocha, C.J.L., Álvarez-Castillo, E., Yáñez, M.R.E., Bengoechea, C., Guerrero, A. and Ledesma, M.T.O., 2020. Development of bioplastics from a microalgae consortium from wastewater. *Journal of Environmental Management*, 263, 110353, https://doi.org/10.1016/j.jenvman.2020.110353.

[16] Shen, M., Song, B., Zeng, G., Zhang, Y., Huang, W., Wen, X. and Tang, W., 2020. Are biodegradable plastics a promising solution to solve the global plastic pollution? *Environmental Pollution*, 263, 114469, https://doi.org/10.1016/j.envpol.2020.114469.

[17] Viera, J.S.C., Marques, M.R.C., Nazareth, M.C., Jimenez, P.C. and Castro, Í.B., 2020. On replacing single-use plastic with so-called biodegradable ones: The case with straws. *Environmental Science and Policy*, 106, 177-181.

[18] Bugnicourt, E., Cinelli, P., Alvarez, V. and Lazzeri, A., 2014. Polyhydroxyalkanoate (PHA): Review of synthesis, characteristics, processing and potential applications in packaging. *Express Polymer Letters*, 8, 791-808.
[19] Shafqat, A., Tahir, A., Mahmood, A., Tabinda, A.B., Yasar, A. and Pugazhendhi, A., 2020. A review on environmental significance carbon foot prints of starch based bio-plastic: A substitute of conventional plastics. *Biocatalysis and Agricultural Biotechnology*, 27, 101540, https://doi.org/10.1016/j.bcab.2020.101540.
[20] RameshKumar, S., Shaiju, P., O'Connor, K.E. and Babu, R., 2020. Bio-based and biodegradable polymers - state-of-the-art, challenges and emerging trends. *Current Opinion in Green and Sustainable Chemistry*, 21, 75-81.
[21] Thakur, S., Chaudhary, J., Sharma, B., Verma, A., Tamulevicius, S. and Thakur, V.K., 2018. Sustainability of bioplastics: Opportunities and challenges. *Current Opinion in Green and Sustainable Chemistry*, 13, 68-75.
[22] Kumar, M., Rathour, R., Singh, R., Sun, Y., Pandey, A., Gnansounou, E., Lin, K.Y.A. and Tsang, D.C.W., 2020. Bacterial polyhydroxyalkanoates: Opportunities, challenges, and prospects. *Journal of Cleaner Production*, 263, 121500, https://doi.org/10.1016/j.jclepro. 2020.121500.
[23] Ng, W.K. and Chow, W.S., 2020. *Plastics in 3D Printing*. *Reference Module in Materials Science and Materials Engineering*. Amsterdam: Elsevier Science.
[24] Bernasconi, R., Natale, G., Levi, M. and Magagnin, L., 2016. Electroless plating of NiP and Cu on polylactic acid and polyethylene terephthalate glycol-modified for 3D printed flexible substrates. *Journal of The Electrochemical Society*, 163(9), D526-D531.
[25] Dixit, N.K., Srivastava, R. and Narain, R., 2017. Electroless metallic coating on plastic parts produced by rapid prototyping technique. *Materials Today: Proceedings*, 4(8), 7643-7653.
[26] Arun, K., Aravindh, K., Raja, K., Jeeva, P.A. and Karthikeyan, S., 2018. Metallization of PLA plastics prepared by FDM-RP process and evaluation of corrosion and hardness characteristics. *Materials Today: Proceedings*, 5(5, Part 2), 13107-13110.
[27] Khan, M.S., Mishra, S.B., Kumar, M.A. and Banerjee, D., 2018. Optimizing surface texture and coating thickness of nickel coated ABS-3D parts. *Materials Today: Proceedings*, 5(9, Part 3), 19011-19018.
[28] Lee, S., Wajahat, M., Kim, J.H., Pyo, J., Chang, W.S., Cho, S.H., Kim, J.T. and Seol, S.K., 2019. Electroless deposition-assisted 3D printing of micro circuitries for structural electronics. *ACS Applied Materials and Interfaces*, 11(7), 7123-7130.
[29] Adachi, H., Taki, K., Nagamine, S., Yusa, A. and Ohshima, M., 2009. Supercritical carbon dioxide assisted electroless plating on thermoplastic polymers. *The Journal of Supercritical Fluids*, 49(2), 265-270.
[30] Wang, M.-Q., Yan, J., Du, S.-G. and Qin, H., 2013. A novel process of electroless nickel plating on PVC with semi-IPN hydrogel pretreatment. *Journal of Alloys and Compounds*, 557, 270-273.
[31] Tamai, T., Watanabe, M., Kobayashi, Y., Nakahara, Y. and Yajima, S., 2017. Surface modification of PEN and PET substrates by plasma treatment and layer-by-layer assembly of polyelectrolyte multilayer thin films and their application in electroless deposition. *RSC Advances*, 7(53), 33155-33161.
[32] Tamai, T., Watanabe, M., Kobayashi, Y., Kobata, J., Nakahara, Y. and Yajima, S., 2019. Surface modification of polyethylene naphthalate substrates by ultraviolet light-irradiation and assembling multilayers and their application in electroless deposition: The chemical and physical properties of the stratified structure. *Colloids and Surfaces A: Physicochemical and Engineering Aspects*, 575, 230-236.

[33] Azim, S.S., Satheesh, A., Ramu, K.K., Ramu, S. and Venkatachari, G., 2006. Studies on graphite based conductive paint coatings. *Progress in Organic Coatings*, 55(1), 1-4.
[34] Jammes, A., Petisme, M. and Staelens, K., 2017. Metallization and selective metallization of silver by spraying. *Surface and Coatings Technology*, 332, 560-563.
[35] Buasri, A., Ongmali, D., Sriboonpeng, P., Prompanut, S. and Loryuenyong, V., 2018. Synthesis of PET-PLA copolymer from recycle plastic bottle and study of its applications in the electrochromic devices with graphene conductive ink. *Materials Today: Proceedings*, 5(5, Part 1), 11060-11067.
[36] Naghdi, S., Rhee, K.Y., Hui, D. and Park, S.J., 2018. A review of conductive metal nanomaterials as conductive, transparent, and flexible coatings, thin films, and conductive fillers: Different deposition methods and applications. *Coatings*, 8(8), https://doi.org/10.3390/coatings8080278.
[37] Andreotti, I.A.A., Orzari, L.O., Camargo, J.R., Faria, R.C., Marcolino-Junior, L.H., Bergamini, M.F., Gatti, A. and Janegitz, B.C., 2019. Disposable and flexible electrochemical sensor made by recyclable material and low cost conductive ink. *Journal of Electroanalytical Chemistry*, 840, 109-116.
[38] Bartolomeo, A.D., Iemmo, L., Urban, F., Palomba, M., Carotenuto, G., Longo, A., Sorrentino, A., Giubileo, F., Barucca, G., Rovere, M., Tagliaferro, A., Ambrosone, G. and Coscia, U., 2019. Graphite platelet films deposited by spray technique on low density polyethylene substrates. *Materials Today: Proceedings*, 20, https://doi.org/10.1016/j.matpr.2019.09.086.
[39] Dehchar, C., Chikouche, I., Kherrat, R., Sahari, A., Zouaoui, A. and Merati, A., 2018. Electroless copper deposition on epoxy glass substrate for electrocatalysis of formaldehyde. *Materials Letters*, 228, 439-442.
[40] Iamsamai, C., Soottitantawat, A., Ruktanonchai, U., Hannongbua, S. and Dubas, S.T., 2011. Simple method for the layer-by-layer surface modification of multiwall carbon nanotubes. *Carbon*, 49(6), 2039-2045.
[41] Rehig, D.L. and Mandich, N.V., 1999. *Throwing Power and Cathode Efficiencies of Gold Electroplating Solutions under Pulse Regimes*. [online] Available at: https://www.nmfrc.org/pdf/p1299b.pdf.
[42] Saviello, D., Andena, L., Gastaldi, D., Toniolo, L. and Goidanich, S., 2018. Multi-analytical approach for the morphological, molecular, and mechanical characterization after photo-oxidation of polymers used in artworks. *Journal of Applied Polymer Science*, 135, 46194, https://doi.org/10.1002/app.46194.
[43] Kurkcu, P., Andena, L. and Pavan, A., 2014. An experimental investigation of the scratch behaviour of polymers-2: Influence of hard or soft fillers. *Wear*, 317(1), 277-290.